Sliding Mode Control With Grid Voltage Modulated Direct Power Control for Three-Phase AC-DC Converter

Gui, Yonghao; Bendtsen, Jan Dimon; Stoustrup, Jakob

Published in:
2019 Chinese Control Conference (CCC)

DOI (link to publication from Publisher):
10.23919/ChiCC.2019.8865280

Publication date:
2019

Document Version
Accepted author manuscript, peer reviewed version

Sliding Mode Control With Grid Voltage Modulated Direct Power Control for Three-Phase AC-DC Converter

Yonghao Gui[1], *Member, IEEE*, Jan Dimon Bendtsen [1], *Member, IEEE*, and Jakob Stoustrup[1], *Senior Member, IEEE*.
1. Department of Electronic Systems, Aalborg University, Aalborg 9220, Denmark
E-mail: yg@es.aau.dk; dimon@es.aau.dk; jakob@es.aau.dk.

Abstract: In this study, a sliding mode control (SMC) based on the grid voltage modulated direct power control (GVM-DPC) is designed for a three-phase pulse-width modulated (PWM) AC-DC converter (rectifier) system. The GVM-DPC method makes the differential active and reactive power equations of the PWM rectifier system transform into a linear time-invariant system from a linear time-varying one. Thus, the conventional linear control techniques consisting of feedback and feedforward controllers are applicable to control active and reactive powers independently. The proposed method is guaranteed that the closed system is globally exponentially stable. In order to maintain a constant dc-link voltage, an SMC method is employed to generate the active power reference of the GVM-DPC method. From the simulation results, the proposed method improves the transient performance of the system and has a robust property to the parameter mismatch.

Key Words: AC-DC converter, grid voltage modulated direct power control, sliding mode control, transient performance.

1 Introduction

Power converters have recently gained tremendous attention due to a broad range of applications such as smart grid, flexible AC transmission systems, renewable energy sources (wind and photovoltaic), and energy storage systems [1–4]. One of the key devices of power converters is a three-phase AC-DC converter (rectifier) with the pulse-width modulation (PWM), which are widely used in various applications, e.g., distributed generation systems, drives of electrical motors, uninterruptible power supplies, etc. [5–7]. One of the most important control objectives of rectifier system is to control its dc-link voltage at a certain constant value.

Normally, two decoupled proportional-integral (PI) controller are designed for the PWM rectifier system in a synchronous rotating reference frame to control *d–q* axes currents independently [8]. The controller designed in the synchronous rotating reference frame has an advantage that it converts the rectifier system from ac signal to dc one. Based on this concept, various control algorithms are applied to the PWM rectifier system, e.g., sliding-mode control (SMC) [9], passivity-based control [10], and model predictive control [11], etc. In order to apply the synchronous rotating reference frame, normally, a phase lock system is used to extract the phase of the grid voltage, which suffers from a slow dynamical response.

To deal with such issue, the method based on direct power control (DPC) is designed through the calculation of active and reactive powers [12]. One of the advantages is that the DPC method eliminates the inner-loop current regulators. However, it obtains a variable switching frequency, which causes a difficulty for the filter design. To overcome such problem, the space vector modulation (SVM) based DPC method is proposed to achieve a constant switching frequency [13, 14]. In addition, the SVM-DPC proposed in [15] obtains a low total harmonics distortion line currents without using positive and negative sequence components under unbalanced grid conditions. In order to obtain an active power oscillation cancellation automatically, a novel definition of reactive power based on pq theory has been applied in DPC strategy [16, 17]. This method provides a constant active power and sinusoidal grid currents even under an unbalanced grid condition. Furthermore, a model predictive control (MPC) based DPC strategy has been applied to power converter applications [11]. The MPC-DPC calculates duty cycles for the rectifier system in every sampling period, i.e., it acheives a constant switching frequency [18]. One of the main problems is that an incorrect voltage sequence selection will adversely affect the converter performance [19]. Moreover, the computation time is a critical issue. Recently, Gui *et al.* introduced a grid voltage modulated (GVM)-DPC algorithm for voltage source converters (VSCs) firstly in [20], and later developed this into a grid-connected voltage source inverter [21]. The main advantage of the GVM-DPC is that it can transform the DPC model of VSCs to a linear time invariant system. That means the various linear technique could be used based on the GVM-DPC technique. Moreover, Gui *et al.* proved that the DPC model with the GVM-DPC is mythically same with the current model in the synchronous rotating reference frame [22]. That means the GVM-DPC concept could be used various applications with consideration its benefits [23–27].

Furthermore. in order to obtain an enhanced dynamic performance of the dc-link voltage, feedforward control techniques have been researched by considering the mismatched power/current disturbances [28, 29]. In addition, to remove the load current sensor on the dc-link for the improvement of the reliability and decrease of the cost, disturbance observers are designed to identify the load current or power disturbance [9, 30]. However, the disturbance observer is not studied in this paper.

Although, the GVM-DPC algorithm was firstly employed to the three-phase rectifier system [24], the input-output linearization (IOL) method is used to control the dc-link voltage. Compared to the work in [24], we modify the GVM-DPC for the ac-side of rectifier system in order to obtain a conventional two second-order system. Then, it is guaranteed that the closed system is globally exponentially stable; Moreover, we use an SMC method to regulate the dc-link voltage in order to enhance the regulation performance compared to the IOL method proposed in [24]. The effectiveness

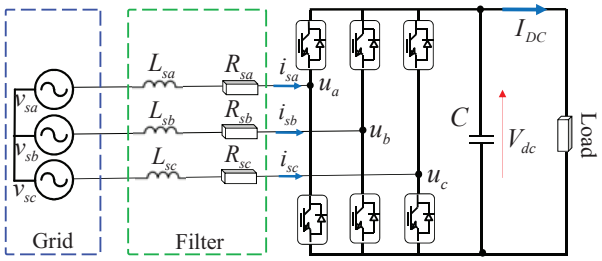

Fig. 1: Three-phase two-level PWM rectifier.

of the proposed method is validated through a simulation using MATLAB/Simulink and PLECS blockset.

The rest of the paper is organized as follows. In Section 2, the model of the rectifier system combining ac and dc side is introduced. In Section 3, we present the design of the modified GVM-DPC and SMC for the dc-link voltage in detail. Section 4 shows the simulation results using MATLAB/Simulink and PLECS blockset. Finally, the conclusions are given in Section 5.

2 Modeling of PWM Rectifier System

Fig. 1 shows the configuration of a typical three-phase two-level PWM rectifier connected to the grid with an L-filter. $v_{s,abc}$, $L_{s,abc}$, $R_{s,abc}$, $i_{s,abc}$, and u_{abc} are the three-phase of grid voltage, filter inductance, filter resistance, line current, and rectifier voltage, respectively. V_{dc} is the voltage at the dc-link, where C is the dc-link capacitor. I_{dc} is the current flowing into the load at the dc-link,

2.1 Model of AC-Side

In this study, we consider a balanced grid voltage, where the relationship between the grid voltage and converter voltage could be described as follows [31]:

$$\begin{aligned} v_{sa} &= R_{sa} i_a + L_{sa} \frac{di_a}{dt} + u_a, \\ v_{sb} &= R_{sb} i_b + L_{sb} \frac{di_b}{dt} + u_b, \\ v_{sc} &= R_{sc} i_c + L_{sc} \frac{di_c}{dt} + u_c. \end{aligned} \tag{1}$$

Assumption 1. *We assume that the filter inductances and resistances of the three phase are the same in this study, i.e., $L_{sa} = L_{sb} = L_{sc} = L_s$ and $R_{sa} = R_{sb} = R_{sc} = R_s$.*

Based on the Clark transformation, the system in (1) is represented in the stationary reference frame as follows:

$$\begin{aligned} v_{s\alpha} &= R_s i_a + L_s \frac{di_\alpha}{dt} + u_\alpha, \\ v_{s\beta} &= R_s i_\beta + L_s \frac{di_\beta}{dt} + u_\beta, \end{aligned} \tag{2}$$

where $v_{s\alpha}$ and $v_{s\beta}$ indicate the grid voltages, $R_{s\alpha}$ and $R_{s\beta}$ indicate filter resistance, $R_{s\alpha}$ and $R_{s\beta}$ indicate filter resistance, i_α and i_β indicate the output currents, and u_α and u_β indicate the rectifier voltages in the stationary reference frame, respectively.

Based on the definition of instantaneous active and reactive powers in the stationary reference frame, we can use the following equations.

$$\begin{aligned} P &= \frac{3}{2}(v_{s\alpha} i_{s\alpha} + v_{s\beta} i_{s\beta}), \\ Q &= \frac{3}{2}(v_{s\beta} i_{s\alpha} - v_{s\alpha} i_{s\beta}), \end{aligned} \tag{3}$$

where P and Q are the injected active and reactive powers of rectifier system, respectively. If we differentiate the injected active and reactive powers of rectifier system in (3) with respect to time, then their variations are expressed such as

$$\begin{aligned} \frac{dP}{dt} &= \frac{3}{2}\left(i_{s\alpha}\frac{dv_{s\alpha}}{dt} + v_{s\alpha}\frac{di_{s\alpha}}{dt} + i_{s\beta}\frac{dv_{s\beta}}{dt} + v_{s\beta}\frac{di_{s\beta}}{dt}\right), \\ \frac{dQ}{dt} &= \frac{3}{2}\left(i_{s\alpha}\frac{dv_{s\beta}}{dt} + v_{s\beta}\frac{di_{s\alpha}}{dt} - i_{s\beta}\frac{dv_{s\alpha}}{dt} - v_{s\alpha}\frac{di_{s\beta}}{dt}\right). \end{aligned} \tag{4}$$

Since we consider a nondistorted grid in this study, we can define the grid voltage in the stationary reference frame as follows:

$$v_{s\alpha} = V_s \cos(\omega t), \quad v_{s\beta} = V_s \sin(\omega t), \tag{5}$$

where V_s indicates the magnitude of $v_{s\alpha,\beta}$ and ω indicates angular frequency of $v_{s\alpha,\beta}$. If we differentiate the grid voltage in (5), then its variations could be expressed such as:

$$\begin{aligned} \frac{dv_{s\alpha}}{dt} &= -\omega V_s \sin(\omega t) = -\omega v_{s\beta}, \\ \frac{dv_{s\beta}}{dt} &= \omega V_s \cos(\omega t) = \omega v_{s\alpha}. \end{aligned} \tag{6}$$

Considering from (2) to (6), we can obtain the dynamics of the injected active and reactive powers of rectifier such as [32]

$$\begin{aligned} \frac{dP}{dt} &= -\frac{R_s}{L_s}P - \omega Q + \frac{3}{2L_s}(v_{s\alpha}u_\alpha + v_{s\beta}u_\beta) - \frac{3}{2L_s}V_s^2, \\ \frac{dQ}{dt} &= \omega P - \frac{R_s}{L}Q + \frac{3}{2L_s}(v_{s\beta}u_\alpha - v_{s\alpha}u_\beta). \end{aligned} \tag{7}$$

where u_α and u_β are the control inputs (rectifier voltages).

Remark 1. *Notice that the dynamics of the injected active and reactive powers in* (7) *describes a time-varying system since the grid voltages multiply by the control inputs.*

2.2 Model of DC-Side

In this study, we neglect the system losses. Thus, the power variation in the dc-link capacitor can be expressed as

$$P_{cap} = CV_{dc}\frac{dV_{dc}}{dt} = P_{rec} - P_{load}, \tag{8}$$

where P_{cap} is the active power stored in the capacitor, P_{rec} is the injected active power of the rectifier system from ac to dc-side, and P_{load} is the consumed power by the load connected in the dc-side. Since we consider a resistor load in this study for the sake of simplicity, P_{load} can be represented such as

$$P_{load} = V_{dc} I_{dc}. \tag{9}$$

Consequelty, the dynamics of the dc-link voltage could be simplified by substituting (9) into (8) such as

$$\frac{dV_{dc}}{dt} = \frac{P_{rec}}{C}\frac{1}{V_{dc}} - \frac{1}{C}I_{dc}. \tag{10}$$

Remark 2. *Notice that the dynamics of the dc-link voltage in* (10) *is nonlinear due to the state in the denominator.*

3 Controller Design for PWM Rectifier

To simplify the controller's design, an LTI system is needed as a system described in the *d-q* frame. To this end, we find a relationship between DPC model and system model in the *d-q* frame.

3.1 Voltage Modulated DPC

In order to obtain an LTI system, we apply the grid voltage modulated (GVM) inputs such as [24]

$$\begin{aligned} u_{GVM1} &= \frac{3}{2L_s}(v_{s\alpha}u_\alpha + v_{s\beta}u_\beta), \\ u_{GVM1} &= \frac{3}{2L_s}(v_{s\beta}u_\alpha - v_{s\alpha}u_\beta). \end{aligned} \tag{11}$$

Then, the dynamics of the injected active and reactive powers of rectifier in (7) is rewritten such as

$$\begin{aligned} \frac{dP}{dt} &= -\frac{R_s}{L_s}P - \omega Q - \frac{3}{2L_s}V_s^2 + u_{GVM1}, \\ \frac{dQ}{dt} &= \omega P - \frac{R_s}{L_s}Q + u_{GVM2}. \end{aligned} \tag{12}$$

Remark 3. *The dynamics of the injected active and reactive powers of rectifier in* (12) *is changed into an LTI system.*

At first, we define that P^* and Q^* are the references of injected active and reactive powers of rectifier, respectively.

Theorem 1. *Consider the system in* (12) *and the controller such as*

$$\begin{aligned} u_{GVM1}. =& \frac{R_s}{L_s}P + \omega Q + \frac{3}{2L_s}V_s^2 + K_{P1}(P^* - P) \\ &+ K_{I1}\int (P^* - P)dt, \\ u_{GVM2}. =& -\omega P + K_{P2}(Q^* - Q) + K_{I2}\int (Q^* - Q)dt, \end{aligned} \tag{13}$$

where K_{P1}, K_{I1}, K_{P2}, and K_{I2} are any positive values; the closed-loop interconnection of the system and controller is exponentially stable. ◊

Proof. At the first step, we define that errors of injected active and reactive powers of rectifier as follows:

$$\begin{aligned} e_P &:= P^* - P, \\ e_Q &:= Q^* - Q, \end{aligned} \tag{14}$$

then, we can obtain error dynamics such as

$$\begin{aligned} \dot{e}_P &= \dot{P}^* - \dot{P}, \\ \dot{e}_Q &= \dot{Q}^* - \dot{Q}. \end{aligned} \tag{15}$$

For the simplicity, we consider the references of injected active and reactive powers of rectifier as constant in this study. Then, substituting (13) into (15), we can obtain the closed-loop system such as

$$\begin{aligned} \dot{e}_P &= K_{P1}e_P + K_{I1}\int e_P dt, \\ \dot{e}_Q &= K_{P2}e_Q + K_{I2}\int e_Q dt. \end{aligned} \tag{16}$$

Let us define the new variables as follows:

$$\begin{aligned} \dot{\psi}_P &= P^* - P, \\ \dot{\psi}_Q &= Q^* - Q. \end{aligned} \tag{17}$$

Then, the whole closed-loop system with (16) and (17) could be represented as follows: Differentiating (16) with respect to time yields

$$\underbrace{\begin{bmatrix} \dot{e}_P \\ \dot{\psi}_P \\ \dot{e}_Q \\ \dot{\psi}_Q \end{bmatrix}}_{\dot{x}} = \underbrace{\begin{bmatrix} -K_{P1} & -K_{I1} & 0 & 0 \\ 1 & 0 & 0 & 0 \\ 0 & 0 & -K_{P2} & -K_{I2} \\ 0 & 0 & 1 & 0 \end{bmatrix}}_{A_{cl}} \underbrace{\begin{bmatrix} e_P \\ \psi_P \\ e_Q \\ \psi_Q \end{bmatrix}}_{x}, \tag{18}$$

where x and A_{cl} are the state and the state-space matrix of the closed-loop system, respectively. If K_{P1}, K_{I1}, K_{P2}, and K_{I2} are positive values, then A_{cl} has all negative eigenvalues. That means the closed-loop system is exponentially stable. □

It is obvious that the closed-loop system consists of two independent second-order systems, which corresponding to the active and reactive power, respectively. The detailed controller gain design process could be found in [24]. In order to obtain the original control inputs (rectifier voltages), we can use the inverse of (11) such as

$$\begin{aligned} u_\alpha &= \frac{2L_s}{3}\frac{v_{s\alpha}u_{GVM1} - v_{s\beta}u_{GVM2}}{V_s^2}, \\ u_\beta &= \frac{2L_s}{3}\frac{v_{s\beta}u_{GVM1} + v_{s\alpha}u_{GVM2}}{V_s^2}. \end{aligned} \tag{19}$$

3.2 DC-Link Controller

In order to control the dc-link voltage at a constant value, we design an SMC method, which is one of best tracking solution. In this study, we neglect the losses between the injected power of the rectifier and dc power.

Let us define a sliding surface s as follows:

$$s = K_{P,V_{dc}}(V_{dc}^* - V_{dc}) + K_{I,V_{dc}}\int (V_{dc}^* - V_{dc})dt, \tag{20}$$

where $K_{P,V_{dc}}$ and $K_{I,V_{dc}}$ are the controller gains. V_{dc}^* is the reference of V_{dc}. On the surface (i.e., $s = 0$), the motion is governed by

$$\dot{K}_{P,V_{dc}}(V_{dc}^* - V_{dc}) + K_{I,V_{dc}}\int (V_{dc}^* - V_{dc})dt = 0 \tag{21}$$

Remark 4. *Choosing $K_{P,V_{dc}} > 0$ and $K_{I,V_{dc}} > 0$ guarantees that the dc-link voltage tends to its reference as the time tends to infinity and the rate of convergence can be determined by the selection of $K_{P,V_{dc}}$ and $K_{I,V_{dc}}$.*

Thus, we can obtain the following equation.

$$\dot{s} = K_{P,V_{dc}}(\dot{V}_{dc}^* - \dot{V}_{dc}) + K_{I,V_{dc}}(V_{dc}^* - V_{dc}), \tag{22}$$

Normally, the dc-link voltage is regulated to a constant value, hence, $\dot{V}_{dc}^* = 0$ in this study.

Theorem 2. *Consider the system in* (10)*, if we take a control law such as*

$$P_{rec} = I_{dc}V_{dc} + \frac{K_{I,V_{dc}}CV_{dc}}{K_{P,V_{dc}}}(V_{dc}^* - V_{dc}) + K_s\mathrm{sat}(\frac{s}{\varepsilon}), \tag{23}$$

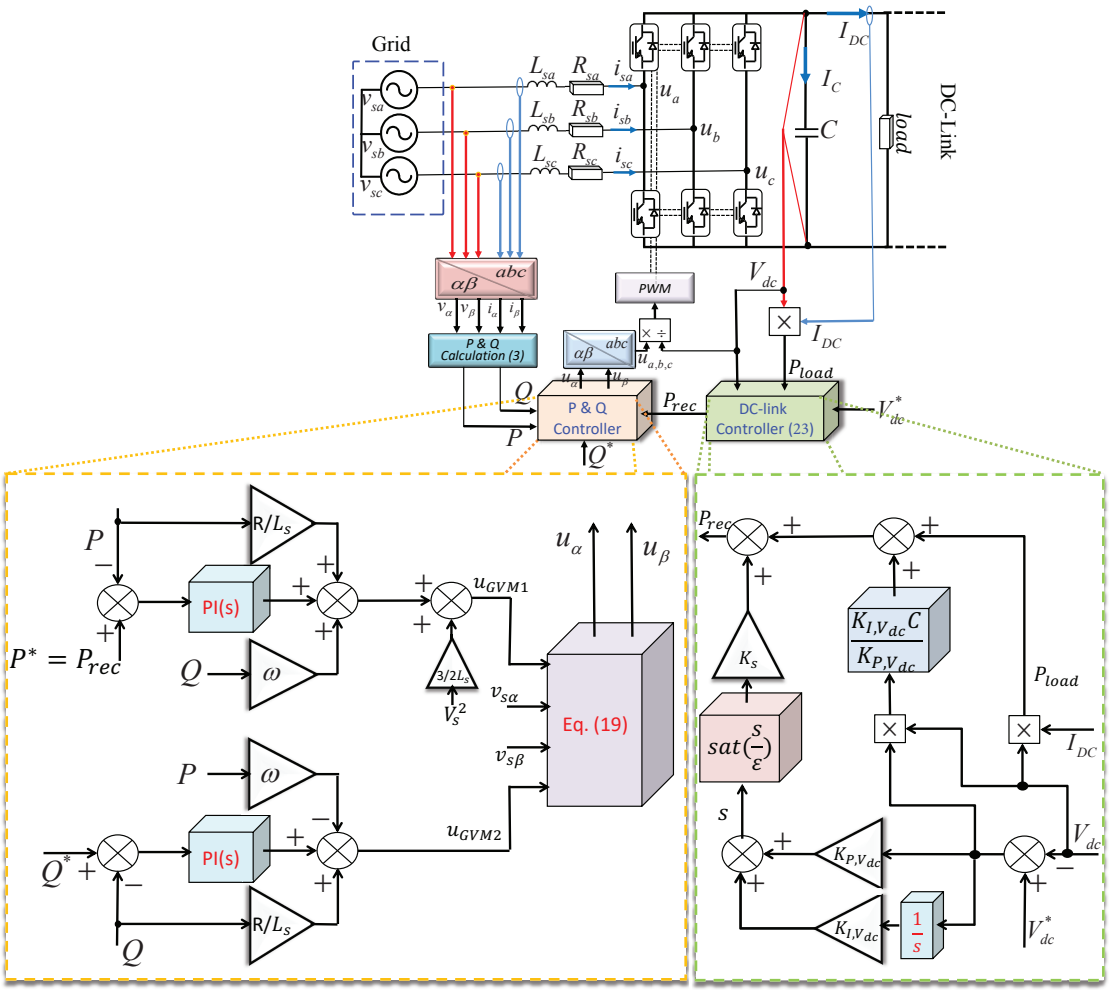

Fig. 2: Block diagram of the proposed method for a two-level PWM rectifier.

where

$$\text{sat}(\frac{s}{\varepsilon}) = \begin{cases} \frac{s}{\varepsilon}, & \text{if } |s| \le |\varepsilon| \\ +1, & \text{if } s > \varepsilon \\ -1, & \text{if } s < -\varepsilon \end{cases},$$

and ε is a positive constant value and taking the controller gain $K_s > 0$, then the trajectory reaches the boundary layer $|s| \le \varepsilon$ in finite time.

Proof. At first, we take a Lyapunov function candidate such as

$$V = \frac{1}{2}s^2. \tag{24}$$

The derivative of Lyapunov function candidate in (24) esults in

$$\begin{aligned} \dot{V} &= s\dot{s} \\ &= s\left[K_{P,V_{dc}}(\dot{V}^*_{dc} - \dot{V}_{dc}) + K_{I,V_{dc}}(V^*_{dc} - V_{dc})\right]. \end{aligned} \tag{25}$$

If we apply a control law in (23), then in $s \ge \varepsilon$, (25) yields

$$\dot{V} = -K_s|s| \tag{26}$$

It is obvious that if $K_s > 0$. then the trajectory reaches the boundary layer $|s| \le \varepsilon$ in finite time. □

Table 1: System parameters used in simulation

Parameter	Symbol	Value	Unit
Nominal grid voltage	$V_{ga,rms}$	110	V
Nominal grid frequency	f	50	Hz
Filter inductance	L	5	mH
Filter resistance	R	0.15	Ω
Dc-link voltage	V_{dc}	500	V
Dc-link capacitance	C	1100	μF
Switching frequency	f_{sw}	10	kHz

Remark 5. *From Theorem 2, we can conclude that the dc-link voltage reaches the boundary layer $|s| \le \varepsilon$ in finite time. After that, the the dc-link voltage will converge to its reference based on $K_{P,V_{dc}}$ and $K_{I,V_{dc}}$.*

It should be noted that the control input, P_{rec} in (23), is generated and sent to the reference of the active power in (13). Consequently, the whole block diagram of the proposed method is shown in Fig. 2.

4 Performance Validation

To validate the proposed SMC of GVM-DPC method, we use MATLAB/Simulink to implement the control algorithm and PLECS blockset to conduct the electrical system. The parameters of the system used in the simulation are listed in

Table 2: Controller gains used in simulation

Methods	$K_{P,V_{dc}}$	$K_{I,V_{dc}}$	K_s	ε
SMC	1	10	200	0.2
IOL	100	1000	-	-

Table 1. The proposed method is compared with the IOL of GVM-DPC proposed in [24]. The controller gains of both method used in the simulation are listed in Table 2.

At first, we compare two methods when the load is connected to dc-link at 0.05 s. Fig. 3 shows the performance of the proposed method and the IOL method. The proposed method has a faster convergence time and a smaller overshoot in the dc-link voltage than the IOL method using 100 times larger gains, as shown in Fig. 3(d). We can observe that the trajectory with the proposed method reaches its sliding surface in the finite time and remains inside the boundary layer. After that, it converges to its equilibrium point smoothly, as shown in Fig. 4. In addition, we also test a case that there is parameter mismatches between the control implementation and real system. Normally, the capacitance of the dc-link capacitor will be decrease after a certain operation time. At this case, we assume that the capacitance in the control implementation has 50% of the nominal value. From Fig. 5, we can observe that the proposed method has the same performance. However, the performance of the IOL method is adversely affected by the parameter mismatch, however.

5 Conclusions

In this paper, we modified the GVM-DPC for three-phase PWM rectifier to control instantaneous active and reactive powers. The SMC is used to obtain the power reference of the ac side in order to maintain the dc-link voltage at a certain value. Simulation results show that the proposed method effectively reduces the overshoot of the dc-link voltage and be robust to the parameter mismatch of the capacitance of the capacitor at the dc-link.

In the future work, a high-order SMC strategy could be considered to avoid the chattering phenomenon. In addition, the disturbance observer of dc-link current will be designed to remove the current sensor for the improvement of the reliability and decrease of the cost.

References

[1] J. Stoustrup, A. Annaswamy, A. Chakrabortty, and Z. Qu, *Smart Grid Control: An Overview and Research Opportunities*. Springer, 2018.

[2] Y. Gui, W. Kim, and C. C. Chung, "Passivity-based control with nonlinear damping for type 2 STATCOM systems," *IEEE Trans. Power Syst.*, vol. 31, no. 4, pp. 2824–2833, 2016.

[3] Q. Sun, J. Zhou, J. M. Guerrero, and H. Zhang, "Hybrid three-phase/single-phase microgrid architecture with power management capabilities," *IEEE Trans. Power Electron.*, vol. 30, no. 10, 2015.

[4] Y. Gui, C. Kim, and C. C. Chung, "Improved low-voltage ride through capability for PMSG wind turbine based on port-controlled Hamiltonian system," *Int. J. Control Autom. Syst.*, vol. 14, no. 5, pp. 1195–1204, 2016.

[5] Y. Li, A. Junyent-Ferré, and J.-M. Rodriguez-Bernuz, "A three-phase active rectifier topology for bipolar DC distribu-

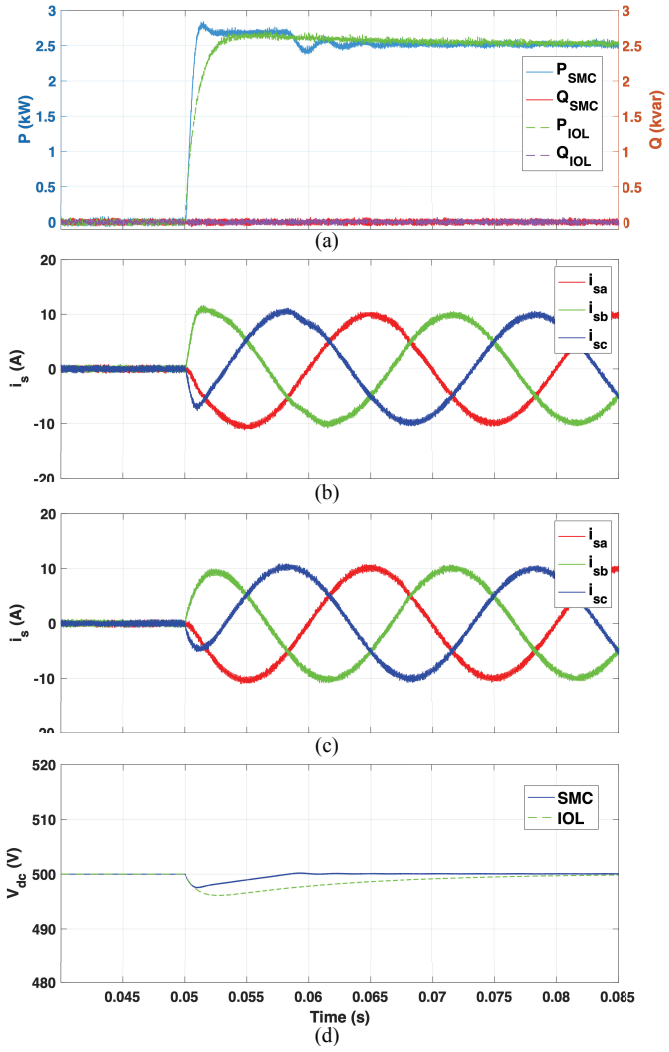

Fig. 3: Simulation results of (a) active and reactive powers, (b) three-phase currents with SMC method, (c) three-phase currents with IOL method, and (d) dc-link voltage.

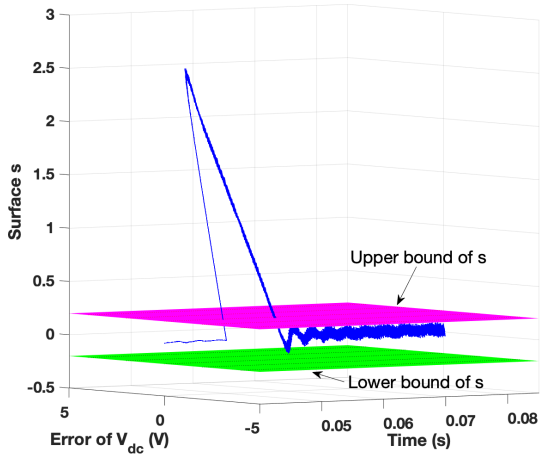

Fig. 4: System trajectory and sliding surface when the load is connected.

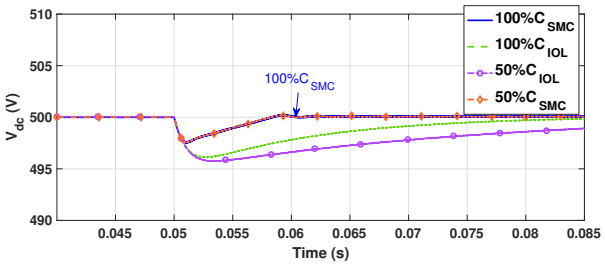

Fig. 5: Dc-link voltage when the capacitance of the dc capacitor has 50% error in the control implementation.

tion," *IEEE Trans. Power Electron.*, vol. 33, no. 2, pp. 1063–1074, 2018.

[6] D. Sun, X. Wang, H. Nian, and Z. Zhu, "A sliding-mode direct power control strategy for DFIG under both balanced and unbalanced grid conditions using extended active power," *IEEE Trans. Power Electron.*, vol. 33, no. 2, pp. 1313–1322, 2018.

[7] B. Wei *et al.*, "Distributed average secondary control for modular UPS systems based microgridss," *IEEE Trans. Power Electron.*, vol. 34, no. 7, pp. 6922–6936, 2018.

[8] M. Kazmierkowski and L. Malesani, "Current control techniques for three-phase voltage-source PWM converters: a survey," *IEEE Trans. Ind. Electron.*, vol. 45, no. 5, pp. 691–703, Oct 1998.

[9] J. Liu, S. Vazquez, L. Wu, A. Marquez, H. Gao, and L. G. Franquelo, "Extended state observer-based sliding-mode control for three-phase power converters," *IEEE Trans. Ind. Electron.*, vol. 64, no. 1, pp. 22–31, 2017.

[10] T.-S. Lee, "Lagrangian modeling and passivity-based control of three-phase AC/DC voltage-source converters," *IEEE Trans. Ind. Electron.*, vol. 51, no. 4, pp. 892–902, 2004.

[11] S. Vazquez et al., "Model predictive control: A review of its applications in power electronics," *IEEE Ind. Electron. Mag.*, vol. 8, no. 1, pp. 16–31, 2014.

[12] T. Noguchi, H. Tomiki, S. Kondo, and I. Takahashi, "Direct power control of PWM converter without power-source voltage sensors," *IEEE Trans. Ind. Appl.*, vol. 34, no. 3, pp. 473–479, 1998.

[13] M. Malinowski, M. Jasiński, and M. P. Kazmierkowski, "Simple direct power control of three-phase PWM rectifier using space-vector modulation (DPC-SVM)," *IEEE Trans. Ind. Electron.*, vol. 51, no. 2, pp. 447–454, 2004.

[14] A. Bouafia, J. Gaubert, and F. Krim, "Predictive direct power control of three-phase pulsewidth modulation (PWM) rectifier using space-vector modulation (SVM)," *IEEE Trans. Power Electron.*, vol. 25, no. 1, pp. 228–236, Jan 2010.

[15] Y. Zhang and C. Qu, "Direct power control of a pulse width modulation rectifier using space vector modulation under unbalanced grid voltages," *IEEE Trans. Power Electron.*, vol. 30, no. 10, pp. 5892–5901, 2015.

[16] ——, "Table-based direct power control for three-phase ac/dc converters under unbalanced grid voltages," *IEEE Trans. Power Electron.*, vol. 30, no. 12, pp. 7090–7099, 2015.

[17] Y. Zhang, J. Gao, and C. Qu, "Relationship between two direct power control methods for PWM rectifiers under unbalanced network," *IEEE Trans. Power Electron.*, vol. 32, no. 5, pp. 4084–4094, 2017.

[18] P. Antoniewicz and M. P. Kazmierkowski, "Virtual-flux-based predictive direct power control of AC/DC converters with online inductance estimation," *IEEE Trans. Ind. Electron.*, vol. 55, no. 12, pp. 4381–4390, 2008.

[19] J. Hu, "Improved dead-beat predictive DPC strategy of grid-connected DC–AC converters with switching loss minimization and delay compensations," *IEEE Trans. Ind. Informat.*, vol. 9, no. 2, pp. 728–738, 2013.

[20] Y. Gui, C. Kim, and C. C. Chung, "Grid voltage modulated direct power control for grid connected voltage source inverters," in *Amer. Control Conf.*, 2017, pp. 2078–2084.

[21] Y. Gui, C. Kim, C. C. Chung, J. M. Guerrero, Y. Guan, and J. C. Vasquez, "Improved direct power control for grid-connected voltage source converters," *IEEE Trans. Ind. Electron.*, vol. 65, no. 10, pp. 8041–8051, Oct 2018.

[22] Y. Gui, X. Wang, F. Blaabjerg, and D. Pan, "Control of grid-connected voltage-source-converters: Relationship between direct-power-control and vector-current-control," *IEEE Ind. Electron. Mag.*, 2019, to be published, DOI: 10.1109/MIE.2019.2898012.

[23] Y. Gui, M. Li, J. M. Guerrero, and J. C. Vasquez, "A novel coordinated control of renewable energy sources and energy storage system in islanded microgrid," in *Amer. Control Conf.*, June 2018, pp. 4616–4621.

[24] Y. Gui, M. Li, J. Lu, S. Golestan, J. M. Guerrero, and J. C. Vasquez, "A voltage modulated DPC approach for three-phase PWM rectifier," *IEEE Trans. Ind. Electron.*, vol. 65, no. 10, pp. 7612–7619, Oct 2018.

[25] Y. Gui, B. Wei, M. Li, J. M. Guerrero, and J. C. Vasquez, "Passivity-based coordinated control for islanded AC microgrid," *Appl. Energy*, vol. 229, pp. 551–561, 2018.

[26] Y. Gui, X. Wang, and F. Blaabjerg, "Vector current control derived from direct power control for grid-connected inverters," *IEEE Trans. Power Electron.*, 2018, to be published, DOI: 10.1109/TPEL.2018.2883507.

[27] Y. Gui, X. Wang, H. Wu, and F. Blaabjerg, "Voltage modulated direct power control for a weak grid-connected voltage source inverters," *IEEE Trans. Power Electron.*, 2019, to be published, DOI: 10.1109/TPEL.2019.2898268.

[28] A. Yazdani and R. Iravani, *Voltage-sourced converters in power systems: modeling, control, and applications*. John Wiley & Sons, 2010.

[29] M. Davari and Y. A.-R. I. Mohamed, "Dynamics and robust control of a grid-connected VSC in multiterminal DC grids considering the instantaneous power of DC-and AC-side filters and DC grid uncertainty," *IEEE Transa. Power Electron.*, vol. 31, no. 3, pp. 1942–1958, 2016.

[30] C. Wang, X. Li, L. Guo, and Y. W. Li, "A nonlinear-disturbance-observer-based DC-bus voltage control for a hybrid AC/DC microgrid," *IEEE Trans. Power Electron.*, vol. 29, no. 11, pp. 6162–6177, 2014.

[31] P. Cortes, J. Rodriguez, P. Antoniewicz, and M. Kazmierkowski, "Direct power control of an AFE using predictive control," *IEEE Trans. Power Electron.*, vol. 23, no. 5, pp. 2516–2523, 2008.

[32] Y. Gui, G. H. Lee, C. Kim, and C. C. Chung, "Direct power control of grid connected voltage source inverters using port-controlled Hamiltonian system," *Int. J. Control Autom. Syst.*, vol. 15, no. 5, pp. 2053–2062, 2017.